HHS Public Access

Author manuscript

Clin Cancer Res. Author manuscript; available in PMC 2019 May 15.

Published in final edited form as:

Clin Cancer Res. 2018 May 15; 24(10): 2408–2416. doi:10.1158/1078-0432.CCR-17-3474.

Androgen Deprivation Therapy Potentiates the Efficacy of Vascular Targeted Photodynamic Therapy of Prostate Cancer Xenografts

Kwanghee Kim[1], **Philip A Watson**[2], **Souhil Lebdai**[1,3], **Sylvia Jebiwott**[1], **Alexander J Somma**[1], **Stephen La Rosa**[1], **Dipti Mehta**[1,4], **Katie S Murray**[5], **Hans Lilja**[4,5,6,7], **David Ulmert**[8], **Sebastien Monette**[9], **Avigdor Scherz**[10], and **Jonathan A Coleman**[5]

[1]Department of Surgery, Memorial Sloan Kettering Cancer Center, New York, NY

[2]Human Oncology and Pathogenesis Program, Memorial Sloan Kettering Cancer Center, New York, NY

[3]Université Pierre and Marie Currie Paris 6, Paris, France

[4]Genitourinary Oncology Service, Department of Medicine, Memorial Sloan Kettering Cancer Center, New York, NY

[5]Division of Urology, Department of Surgery, Memorial Sloan Kettering Cancer Center, New York, NY

[6]Department of Laboratory Medicine, Memorial Sloan Kettering Cancer Center, New York, NY

[7]Nuffield Department of Surgical Sciences, University of Oxford, Oxford, UK

[8]Molecular Pharmacology Program, Memorial Sloan Kettering Cancer Center, New York, NY

[9]Laboratory of Comparative Pathology, Memorial Sloan Kettering Cancer Center, Rockefeller University, Weill Cornell Medicine, New York, NY

[10]Department of Plants and Environmental Sciences, The Weizmann Institute of Science, Rehovot, Israel

Abstract

Purpose—WST11 vascular targeted photodynamic therapy (VTP) is a local ablation approach relying upon rapid, free radical-mediated destruction of tumor vasculature. A phase III trial showed that VTP significantly reduced disease progression when compared to active surveillance in patients with low-risk prostate cancer (PCa). The aim of this study was to identify a druggable pathway that could be combined with VTP to improve its efficacy and applicability to higher risk PCa tumors.

Corresponding Author: Jonathan A Coleman, [5]Division of Urology, Department of Surgery, Memorial Sloan Kettering Cancer Center, New York, NY10065. Phone: 646-422-4432; colemanj@mskcc.org.

The authors declare no potential conflicts of interest

Experimental design—Transcriptome analysis of VTP treated tumors (LNCaP-AR xenografts) was used to identify a candidate pathway for combination therapy. The efficacy of the combination therapy was assessed in mice bearing LNCaP-AR or VCaP tumors.

Results—Gene Set Enrichment Analysis (GSEA) identifies the enrichment of androgen responsive gene sets within hours post-VTP treatment, suggesting that the androgen receptor (AR) may be a viable target in combination with VTP. We tested this hypothesis in mice bearing LNCaP-AR xenograft tumors by using androgen deprivation therapy (ADT), degarelix, in combination with VTP. Compared to either ADT or VTP alone, a single dose of degarelix in concert with VTP significantly inhibited tumor growth. A sharp decline in serum PSA confirmed AR inhibition in this group. Tumors treated by VTP and degarelix displayed intense TUNEL staining 7 days post-treatment, supporting an increased apoptotic frequency underlying the effect on tumor inhibition.

Conclusion—Improvement of local tumor control following androgen deprivation combined with VTP provides the rationale and preliminary protocol parameters for clinical trials in patients presented with locally advanced PCa.

Keywords

androgen deprivation therapy; prostatic neoplasm; WST11; VTP

Introduction

Current treatment choices for localized PCa range from active surveillance to radical therapies (prostatectomy, external beam radiation) (1). However, active surveillance can present a risk of progression for patients with higher-risk disease, while for some cancers, radical therapies may be an unnecessarily aggressive overtreatment and are associated with notable side effects (2–4). Therefore, there has been interest in developing partial gland ablation such as focal therapies that are less aggressive than radical therapies as an alternative treatment option for these patients (5). VTP destroys targeted tissues using padeliporfin (TOOKAD® Soluble, WST11) as a photosensitizer in association with a low power near-infrared laser light in the presence of oxygen. Padeliporfin is intravenously infused and circulates systemically with no extravagation out of the circulation until clearance. Illumination confined to the cancerous lobe of the prostate using transperineal optic fibers induces ultrafast electron transfer to oxygen molecules in the circulation. The resulting short lived super oxide and hydroxyl radicals (6, 7) initiate rapid destruction of the targeted vasculature followed by a cascade of biological events that end with coagulative necrosis of the tumor (6–8).

Positive outcomes from patients with low-risk, localized PCa [Grade Group 1 (Gleason Score≤ 6), no prior treatment] treated with VTP have recently been reported in U.S. and European multi-center phase II and III studies. In follow up biopsies at 6 months after prostate hemiablation, up to 80.6% of patients were negative for cancer (9) and there was a decreased disease progression at 24 months when compared to active surveillance (28% versus 58% respectively, HR 0.34, 95%CI 0.24–0.46; p<0.0001) (10). After a median follow-up of 68 months, 82% of patients treated with VTP were free of clinically significant

cancer in the treated lobes and 76% of the treated patients had avoided a need for subsequent radical therapy (11). The efficacy of VTP could potentially be improved with a complementary, targeted combination therapy. Furthermore, combination therapy may allow for the extension of VTP treatment to additional cohorts of patients with high-risk localized PCa.

The initial aim of this study was therefore to identify potential druggable pathways active in PCa tumors exposed to VTP using transcriptome analysis. We identified a compensatory, acute upregulation of AR pathway activation following VTP treatment. As ADT to inhibit pro-survival signaling via AR is the mainstay treatment for aggressive PCa, we then went on to confirm that inhibition of AR activity enhanced the efficacy of VTP treatment in PCa xenograft models.

Material and methods

General

Lyophilized WST11 was obtained from Steba Biotech (Cedex, France). Human prostate cancer cell lines VCaP was purchased from ATCC (Manassas, VA) and LNCaP-AR was kindly provided by Dr. Charles Sawyers (MSKCC), respectively. Both cell lines were tested negative for mycoplasma using the MycoAlert™ PLUS Assay from Lonza (Basel, Switzeland). LNCaP-AR cells were cultured in RPMI supplemented with 10% FBS, 2 mmol/L L-glutamine while VCaP cells were cultured in DMEM with high glucose,10% FBS and 2 mmol/L L-glutamine. All the components for cell culture were from Life Technologies (Grand Island, NY). Degarelix was purchased from Ferring Pharmaceuticals Inc. (Parsippany, NJ).

Animal models

All animal work was performed in accordance with a protocol approved by the IACUC of Memorial Sloan Kettering Cancer Center. Subcutaneous tumors were established in intact male mice through injection of LNCaP-AR or VCaP human prostate cancer cell lines. We subcutaneously injected $2x10^6$ LNCaP-AR cells in 100 μL of 1:1 media/Matrigel (BD Biosciences, San Jose, CA) into the hindlimb area of 6–8 week old, male, athymic nude mice (NCI, Fredrick, MD) or SCID mice (C.B-*Igh-1*^{b}/IcrTac-*Prkdc*^{scid}, Taconic, Hudson, NY). We also injected $2x10^6$ VCaP cells into SCID mice (Taconic). Tumor growth was monitored by caliper measurement weekly. When the volume of tumors reached approximately 100 mm^3, the animals were randomly assigned to different cohorts for further experiments.

Treatments

VTP—An anesthetic cocktail of 150 mg/kg ketamine and 10 mg/kg xylazine was administered intraperitoneally prior to treatment and was supplemented with inhaled isoflurane. A single dose of carprofen (5 mg/kg) and 1 mL of subcutaneous warm saline were administered. WST11 was reconstituted in sterile 5% dextran in water at 2 mg/mL under light protected condition and the aliquots were stored at −20°C. On the day of VTP treatment, an aliquot was thawed and filtered through 0.2 μm disc syringe filter (Sartorius

Stedin Biotech North America, Bohemia, NY). The mice were intravenously infused with WST11 via tail vein (9 mg/kg) followed immediately by 10 minutes laser (Ceramoptec, Bonn, Germany) illumination (755 nm, 100 mW/cm for transcriptome analyses and 150 mW/cm for in vivo studies) through a 1 mm frontal fiber (MedLight S.A., Ecublens, Switzerland). The light field was arranged to cover the entire tumor area plus 1 mm rim using red-light aiming beam.

ADT—Single dose of degarelix was administered at 0.5 mg per mouse at 3 days before VTP treatment via subcutaneous or intraperitoneal injection. Drug administration was initiated when tumor size reached ~100 mm^3.

PSA detection in serum

Free PSA and total PSA were measured with a dual-label immunofluorometric assay (DELFIA Prostatus™ PSA Free/Total PSA; Perkin-Elmer Life Sciences) according to the manufacturer's recommendations. This assay measures free PSA and complexed PSA in an equimolar fashion (12, 13), and the cross-reactivity of PSA-ACT for free PSA is less than 0.2% (14). The lower limits of detection are 0.1 ng/mL for both total PSA and free PSA. For detection, the 1235 automatic immunoassay system from Perkin-Elmer Life Sciences (Waltham, MA) was used.

Histology and immunohistochemistry

All tumor specimens were fixed in 10% buffered formalin (Fisher Scientific, Pittsburgh, PA), processed routinely, embedded in paraffin, sectioned at 5-micron thickness, and stained with hematoxylin-eosin (H&E). Immunohistochemistry (IHC) of tumors was performed on 5 micron formalin-fixed paraffin embedded (FFPE) section following heat induced epitope retrieval (HIER) in a buffer at pH 9.0. AR staining with anti-AR antibody (at 0.66 μg/ml, Abcam, Cambridge, MA) and TUNEL staining for cell death with terminal deoxynucleotidyl transferease dUTP nick-end labeling (Roche Diagnostics, Indianapolis, IN) was performed using Discovery XT processor (Ventana Medical Systems, Inc., Tucson, AZ) (15) at the Molecular Cytology core facility. IHC staining for CD31 and Ki67 markers was performed on FFPE sections at the Laboratory of Comparative Pathology on a Leica Bond RX automated stainer (Leica Biosystems, Buffalo Grove, IL). Following HIER at pH 9.0, the primary antibody against CD31 (DIA-310, Dianova, Hamburg, Germany) or Ki67 (ab16667, Abcam, Cambridge, MA) was applied at a concentration of 1:250 and 1:100 respectively, followed by application of a polymer detection system (DS9800, Novocastra Bond Polymer Refine Detection, Leica Biosystems). For all IHC stains and TUNEL, the chromogen was 3,3 diaminobenzidine tetrachloride (DAB), and sections were counterstained with haematoxylin. For quantification of CD31, Ki67 and TUNEL staining, whole slide digital images were generated on a scanner (Pannoramic 250 Flash III, 3DHistech, 20x/0.8NA objective, Budapest, Hungary) at a resolution of 0.2431 μm per pixel. Staining quantification was performed with QuPath 0.1.2 software (Centre for Cancer Research & Cell Biology, Queen's University Belfast, UK). For CD31 and Ki67, the region of interest (ROI) was defined as viable tumor tissue excluding necrosis. For TUNEL, the ROI was defined as total tumor tissue including necrosis. For CD31 and TUNEL, the positive area, defined as the ratio of DAB stained pixels to total ROI area, was measured using the positive

pixel count algorithm. For Ki67, the ratio (percentage) of cells with positive nuclear staining to total cell number was measured with the positive cell detection algorithm. ROI selection, algorithm optimization and validation, and qualitative examination of H&E slides, were performed by a board-certified veterinary pathologist (SM).

GSEA for transcriptome analysis of LNCaP-AR xenografts following VTP treatment

LNCaP-AR xenografts were established in intact SCID mice by injecting 2 million cells as described previously (16) and, once established, were treated with VTP at 9 mg/kg WST11 followed by 100 mW laser fluence. Tumors were collected at 3, 6, or 24 hours, 1 week and 8.5 weeks post VTP and RNA was isolated following the standard protocol using TRIzol (Fisher Scientific). Expression profiling was performed using Illumina HT-12 Expression BeadChip array and the data was analyzed using Partek Genomics Suite (Partek Inc., St. Louis, MO). The microarray data then underwent secondary analysis by GSEA (17) using gene sets from the Hallmark and C2, Canonical Pathways collections (Molecular Signature Databases v6.0 (MSigDB); Broad Institute: http://software.broadinstitute.org/gsea/msigdb). GSEA| MSigDB. Accessed 19 Jun 2017. Microarray data has been deposited in the National Center for Biotechnology Information Gene Expression Omnibus (GEO) (GSE109681).

Statistical analysis

Two-way ANOVA test using GraphPad Prism (GraphPad Software, La Jolla, CA) was used for therapeutic efficacy in affecting tumor growth, and One-way ANOVA for PSA and a Mann-Whitney test for CD31, Ki67 or TUNEL staining quantification. Differences with p values < 0.05 were considered statistically significant.

Results

Transcriptome analysis of VTP-treated tumors by GSEA revealed an enrichment of androgen response pathways

To identify potential druggable pathways active in PCa that could be exploited for combination therapy with VTP, we analyzed the transcriptome of LNCaP-AR xenograft tumors following acute VTP exposure. Unbiased GSEA identified statistically significant enrichments with gene sets related to hypoxia, HIF1A, and VEGFR pathways at three to six hours post-VTP treatment (Figure 1, Supplementary Table S1/2), effects that have previously been shown to be associated with photodynamic therapies (PDT) (18). Interestingly, AR signaling gene sets were also up-regulated in VTP-treated tumors compared to control mice, suggesting that the AR may be a viable target for combination therapy with VTP.

Combination therapy of ADT with VTP suppressed tumor growth to a greater extent than either treatment alone

To test our hypothesis that the preemptive blocking of androgen signaling upregulation induced by VTP might improve the outcome of tumor growth control, we tested the combination of VTP with an androgen signaling pathway inhibitor in widespread clinical use for the treatment of PCa. Degarelix is a long-acting, gonadotropin-releasing hormone antagonist that results in a rapid onset of medical castration (19, 20). To establish preexisting AR inhibition, treatment with degarelix was initiated three days prior to administering VTP

to PCa xenograft tumors. Prior studies with VTP established that components of the immune response contributed to the anticancer activity of VTP (21). We therefore compared the efficacy of the combination therapy against LNCaP-AR tumors in both athymic nude (T cell deficient) (Figure 2A) and severe combined immunodeficiency (SCID) (both T and B cell deficient) (Figure 2B) mice. Tumor bearing nude mice were randomly assigned to four cohorts: control, degarelix, VTP, and degarelix and VTP combination. The combination of degarelix and VTP resulted in statistically significant improved tumor growth control compared to either degarelix ($p<0.01$) or VTP alone ($p<0.005$) (Figure 2A). As in the nude mouse, the combination of degarelix and VTP led to superior control of LNCaP-AR tumor growth in SCID mice ($p<0.0001$ for either monotherapy vs. combination) (Figure 2B). The combination of degarelix and VTP was also significantly more effective than VTP alone ($p<0.005$) or degarelix alone ($p<0.0001$) (Figure 3) in delaying the growth of VCaP, a human PCa model with AR gene amplification that also expresses the constitutively active AR splice variant, AR-V7.

Combination therapy of ADT and VTP was more effective than VTP alone in downregulation of total PSA levels and induction of apoptosis/necrosis

To verify that AR activity was inhibited by the treatments, we measured the levels of total PSA (tPSA) in serum of mice bearing LNCaP-AR tumors (Figure 4A). tPSA values were determined in separate cohorts of mice at one, three, or seven days post-VTP (four, six or ten days post-degarelix). tPSA values declined by either VTP or degarelix alone, but the sharpest drop in tPSA levels was seen with the combination of degarelix and VTP ($p<0.05$ vs. control across all time points).

In parallel, we assessed the histology of degarelix and/or VTP treated tumors on days three and seven post-VTP by both hematoxylin/eosin and TUNEL assay to detect cell death (apoptotic and/or necrotic cells) (Figure 4B). VTP treated tumors displayed partial cell death characterized by large foci of TUNEL staining, but with significant TUNEL negative areas. Tumors treated with combination therapy appeared to display more extensive areas of TUNEL staining. Although not statistically significant compared to VTP alone, there were fewer tumors that escaped cell death in the combination group, suggesting that increased cell death underlies the effect on tumor inhibition. In contrast, degarelix alone treated tumors exhibited little TUNEL staining, but still showed reduced Ki67 signal compared to controls, as expected ($p<0.05$, Supplemental Figure 1). These findings are reminiscent of patient studies, which have reported overall low frequencies of apoptosis in PCa following ADT (22, 23). Nuclear AR staining was inversely correlated with TUNEL, suggesting that viable AR-positive cells had escaped focal therapy effects of VTP alone. Notably, the tumors treated with combination therapy were absent of AR staining, suggesting that remaining viable tumor cells were few in number.

ADT reduces tumor vessel staining

CD31 is primarily a marker for endothelial cells which can help evaluate the degree of intratumoral vessel formation. The degarelix treated tumors appear to have less vessels than tumors in the control group as shown in Figure 5A. The quantification of staining area depicts a 38% decrease in CD31 in degarelix-treated tumors compared to tumors ($p<0.05$) in

the control group. This might be a contributing factor of reduction in tumor recurrence in ADT/VTP combination group, although we did not observe any significant difference in CD31 vessel counts between the combination and VTP groups with the caveat that there was minimal remaining viable tumor material in these two groups (Supplemental Figure 2).

Discussion

The effective adoption of prostate cancer screening has led to earlier detection of small, clinically significant prostate cancers amenable to the newly developed treatment strategies for partial gland ablation which are well tolerated and associated with fewer adverse side effects than aggressive radical therapies such as surgery and radiation. Positive oncologic outcomes in clinical studies of VTP has led to the recent approval of TOOKAD® Soluble for the treatment of low-risk PCa and highlights the potential of VTP to serve as an alternative to active surveillance or radical therapies (9–11). To potentially extend VTP treatment to larger cohorts of patients, we have recently launched a VTP clinical trial (NCT03315754) for patients with localized PCa of intermediate risk, Grade Group 2 [Gleason score 7 (3+4)]. However, adaptation of this treatment to slightly larger and more aggressive tumors has potential risk for under-treatment, prompting the need for augmenting the mechanism of VTP mediated tissue necrosis.

A byproduct of the oxidative damage triggered by photodynamic therapies (PDT) is the induction of intrinsic cellular stress response pathways, and these are thought to contribute to cancer cell survival and therapy resistance (18). To identify stress response pathways amendable to pharmaceutical intervention that could be used in conjunction with VTP, we performed transcriptome and gene set enrichment analyses of VTP treated human prostate xenograft tumors. Consistent with earlier studies of PDT in cancer (18), we observed the upregulation of gene sets related to hypoxia/HIF1-α, VEGFR, AP-1, and NF-κB in the immediate hours following VTP exposure. Additionally, other potential cell survival pathways such as EGF/EGFR were also enriched post-VTP. Although EGFR inhibitors (erlotinib, gefitinib, lapatinib) have been clinically evaluated for prostate cancer, these phase II trials were limited to those with advanced or metastatic disease and displayed clinical benefit in only a small subset of patients [lapatinib (24, 25), erlotinib (26, 27), gefitinib (28)]. However, of particular interest to our study was the finding that VTP treatment resulted in the acute upregulation of pathways related to AR signaling. Targeted AR inhibition forms the cornerstone of therapy for metastatic PCa (29), and is the standard of care in the neoadjuvant or adjuvant setting for high risk localized disease treated with external-beam radiotherapy (EBRT) (30). AR inhibition is also being increasingly explored in clinical trials as neoadjuvant or adjuvant treatment for surgical patients with intermediate to high risk localized prostate cancer. Thus, there is supporting rationale for targeting AR in the setting of VTP mediated tissue ablation for PCa.

ADT can be accomplished by orchiectomy, but is more commonly achieved medically through the use of gonadotropin-releasing hormone (GnRH) agonists (leuprolide, goserelin, triptorelin) or more recently, antagonists (degarelix). GnRH agonists are known to cause an initial surge in circulating testosterone levels before achieving castration levels. In contrast, degarelix results in rapid castration in both men and mice without the testosterone flare (31,

32). In nude mice, a GnRH antagonist modestly outperformed an agonist in growth inhibition of a prostate cancer xenograft (33).

We chose degarelix to test the hypothesis that neoadjuvant ADT may improve anti-tumor efficacy of VTP in mice bearing prostate cancer xenograft tumors. In multiple model systems, the combination of degarelix and VTP offered superior local tumor growth inhibition compared to either degarelix or VTP alone. The combination treated group displayed fewer tumors that escaped cell death compared to VTP alone. We did not detect a substantial induction of apoptosis in the tumors treated with degarelix alone, which is consistent with clinical reports demonstrating that PCa apoptosis is not commonly seen in patients after ADT (22, 23). Treatment success was also demonstrated by AR inhibition that was reflected in the significant reduction in serum PSA levels, which was most extensive in the combination group.

Induction of tumor hypoxia following photodynamic therapy with subsequent activation of cellular survival pathways and angiogenesis are potential factors that could adversely impact VTP treatment response (18). In prostate cancer cells, androgens promote the expression of HIF1-α and VEGF (34, 35), and HIF1-α enhances the activity of AR signaling (36, 37). Thus, the hypoxic tumor microenvironment induced by VTP with corresponding HIF1-α upregulation could result in promotion of pro-tumorigenic AR signaling, which is consistent with the results of our gene set analysis. Studies in PCa patients have demonstrated that tumor hypoxia and HIF1-α are decreased following ADT (38, 39). In PCa model systems, ADT decreases VEGF production and reduces tumor vascularization (40–42) corresponding to the decrease in CD31-positive staining of endothelial cells following degarelix treatment in this study. Thus, we propose that ADT potentiates the efficacy of VTP treatment at least in part by counterbalancing the pro-tumorigenic effects of hypoxia and angiogenesis.

Our findings draw parallels with the use of neoadjuvant and adjuvant ADT in combination with EBRT, which was first demonstrated 20 years ago to extend survival in patients with locally advanced PCa (43, 44). If the combination of ADT and VTP is found effective in the clinical setting, this strategy may provide means for effective treatment of locally advanced PCa with significantly less side effects than the current approaches.

Supplementary Material

Refer to Web version on PubMed Central for supplementary material.

Acknowledgments

Authors thank Thompson Family Foundation (KK, SL, SJ, AJS, SLR, KSM, AS, JAC), MSKCC Molecular Cytology Core Facility and the Laboratory of Comparative Pathology. Contributions from core facilities were supported in part by NIH/NCI Cancer Center Support Grant P30 CA008748. LH is supported in part by a Cancer Center Support Grant from the National Institutes of Health/National Cancer Institute (NIH/NCI) made to Memorial Sloan Kettering Cancer Center [P30 CA008748], the MSKCC SPORE in Prostate Cancer (P50CA092629), the Sidney Kimmel Center for Prostate and Urologic Cancers, David H. Koch through the Prostate Cancer Foundation, and Oxford Biomedical Research Centre Program in UK.

References

1. Heidenreich A, Bastian PJ, Bellmunt J, Bolla M, Joniau S, van der Kwast T, et al. EAU guidelines on prostate cancer. part 1: screening, diagnosis, and local treatment with curative intent-update 2013. Eur Urol. 2014; 65:124–37. [PubMed: 24207135]
2. Garisto JD, Klotz L. Active Surveillance for Prostate Cancer: How to Do It Right. Oncology (Williston Park). 2017; 31:333–40. 345. [PubMed: 28512731]
3. Wilt TJ, Brawer MK, Jones KM, Barry MJ, Aronson WJ, Fox S, et al. Radical prostatectomy versus observation for localized prostate cancer. N Engl J Med. 2012; 367:203–13. [PubMed: 22808955]
4. Hamdy FC, Donovan JL, Lane JA, Mason M, Metcalfe C, Holding P, et al. 10-Year Outcomes after Monitoring, Surgery, or Radiotherapy for Localized Prostate Cancer. N Engl J Med. 2016; 375:1415–24. [PubMed: 27626136]
5. Cathelineau X, Sanchez-Salas R. Focal Therapy for Prostate Cancer: Pending Questions. Curr Urol Rep. 2016; 17:86. [PubMed: 27761805]
6. Ashur I, Goldschmidt R, Pinkas I, Salomon Y, Szewczyk G, Sarna T, et al. Photocatalytic generation of oxygen radicals by the water-soluble bacteriochlorophyll derivative WST11, noncovalently bound to serum albumin. J Phys Chem A. 2009; 113:8027–37. [PubMed: 19545111]
7. Brandis A, Mazor O, Neumark E, Rosenbach-Belkin V, Salomon Y, Scherz A. Novel water-soluble bacteriochlorophyll derivatives for vascular-targeted photodynamic therapy: synthesis, solubility, phototoxicity and the effect of serum proteins. Photochem Photobiol. 2005; 81:983–93. [PubMed: 15839743]
8. Borle F, Radu A, Fontolliet C, van den Bergh H, Monnier P, Wagnières G. Selectivity of the photosensitiser Tookad for photodynamic therapy evaluated in the Syrian golden hamster cheek pouch tumour model. Br J Cancer. 2003; 89:2320–26. [PubMed: 14676813]
9. Azzouzi AR, Barret E, Bennet J, Moore C, Taneja S, Muir G, et al. TOOKAD® Soluble focal therapy: pooled analysis of three phase II studies assessing the minimally invasive ablation of localized prostate cancer. World J Urol. 2015; 33:945–53. [PubMed: 25712310]
10. Azzouzi A-R, Vincendeau S, Barret E, Cicco A, Kleinclauss F, van der Poel HG, et al. Padeliporfin vascular-targeted photodynamic therapy versus active surveillance in men with low-risk prostate cancer (CLIN1001 PCM301): an open-label, phase 3, randomised controlled trial. Lancet Oncol. 2017; 13:181–91.
11. Lebdai S, Bigot P, Leroux P-A, Berthelot L-P, Maulaz P, Azzouzi A-R. Vascular Targeted Photodynamic Therapy with Padeliporfin for Low Risk Prostate Cancer Treatment: Midterm Oncologic Outcomes. J Urol. 2017; doi: 10.1016/j.juro.2017.03.119
12. Ulmert D, Evans MJ, Holland JP, Rice SL, Wongvipat J, Pettersson K, et al. Imaging androgen receptor signaling with a radiotracer targeting free prostate-specific antigen. Cancer Discov. 2012; 2:320–27. [PubMed: 22576209]
13. Mitrunen K, Pettersson K, Piironen T, Björk T, Lilja H, Lövgren T. Dual-label one-step immunoassay for simultaneous measurement of free and total prostate-specific antigen concentrations and ratios in serum. Clin Chem. 1995; 41:1115–20. [PubMed: 7543033]
14. Pettersson K, Piironen T, Seppälä M, Liukkonen L, Christensson A, Matikainen MT, et al. Free and complexed prostate-specific antigen (PSA): in vitro stability, epitope map, and development of immunofluorometric assays for specific and sensitive detection of free PSA and PSA-alpha 1-antichymotrypsin complex. Clin Chem. 1995; 41:1480–88. [PubMed: 7586521]
15. Gavrieli Y, Sherman Y, Ben-Sasson SA. Identification of programmed cell death in situ via specific labeling of nuclear DNA fragmentation. J Cell Biol. 1992; 119:493–501. [PubMed: 1400587]
16. Chen CD, Welsbie DS, Tran C, Baek SH, Chen R, Vessella R, et al. Molecular determinants of resistance to antiandrogen therapy. Nat Med. 2004; 10:33–39. [PubMed: 14702632]
17. Subramanian A, Tamayo P, Mootha VK, Mukherjee S, Ebert BL, Gillette MA, et al. Gene set enrichment analysis: a knowledge-based approach for interpreting genome-wide expression profiles. Proc Natl Acad Sci U S A. 2005; 102:15545–50. [PubMed: 16199517]
18. Broekgaarden M, Weijer R, van Gulik TM, Hamblin MR, Heger M. Tumor cell survival pathways activated by photodynamic therapy: a molecular basis for pharmacological inhibition strategies. Cancer Metastasis Rev. 2015; 34:643–90. [PubMed: 26516076]

19. Broqua P, Riviere PJ-M, Conn PM, Rivier JE, Aubert ML, Junien J-L. Pharmacological profile of a new, potent, and long-acting gonadotropin-releasing hormone antagonist: degarelix. J Pharmacol Exp Ther. 2002; 301:95–102. [PubMed: 11907162]
20. Klotz L, Boccon-Gibod L, Shore ND, Andreou C, Persson B-E, Cantor P, et al. The efficacy and safety of degarelix: a 12-month, comparative, randomized, open-label, parallel-group phase III study in patients with prostate cancer. BJU Int. 2008; 102:1531–8. [PubMed: 19035858]
21. Preise D, Oren R, Glinert I, Kalchenko V, Jung S, Scherz A, et al. Systemic antitumor protection by vascular-targeted photodynamic therapy involves cellular and humoral immunity. Cancer Immunol Immunother. 2009; 58:71–84. [PubMed: 18488222]
22. Westin P, Stattin P, Damber JE, Bergh A. Castration therapy rapidly induces apoptosis in a minority and decreases cell proliferation in a majority of human prostatic tumors. Am J Pathol. 1995; 146:1368–75. [PubMed: 7778676]
23. Colecchia M, Frigo B, Del Boca C, Guardamagna A, Zucchi A, Colloi D, et al. Detection of apoptosis by the TUNEL technique in clinically localised prostatic cancer before and after combined endocrine therapy. J Clin Pathol. 1997; 50:384–8. [PubMed: 9215120]
24. Whang YE, Armstrong AJ, Rathmell WK, Godley PA, Kim WY, Pruthi RS, et al. A phase II study of lapatinib, a dual EGFR and HER-2 tyrosine kinase inhibitor, in patients with castration-resistant prostate cancer. Urol Oncol. 2013; 31:82–6. [PubMed: 21396844]
25. Liu G, Chen YH, Kolesar J, Huang W, Dipaola R, Pins M, et al. Eastern Cooperative Oncology Group Phase II Trial of lapatinib in men with biochemically relapsed, androgen dependent prostate cancer. Urol Oncol. 2013; 31:211–8. [PubMed: 21784672]
26. Nabhan C, Lestingi TM, Galvez A, Tolzien K, Kelby SK, Tsarwhas D, et al. Erlotinib has moderate single-agent activity in chemotherapy-naïve castration-resistant prostate cancer: final results of a phase II trial. Urology. 2009; 74:665–71. [PubMed: 19616281]
27. Gravis G, Bladou F, Salem N, Gonçalves A, Esterni B, Walz J, et al. Results from a monocentric phase II trial of erlotinib in patients with metastatic prostate cancer. Ann Oncol. 2008; 19:1624–8. [PubMed: 18467313]
28. Pezaro C, Rosenthal MA, Gurney H, Davis ID, Underhill C, Boyer MJ, et al. An open-label, single-arm phase two trial of gefitinib in patients with advanced or metastatic castration-resistant prostate cancer. Am J Clin Oncol. 2009; 32:338–41. [PubMed: 19363437]
29. Watson PA, Arora VK, Sawyers CL. Emerging mechanisms of resistance to androgen receptor inhibitors in prostate cancer. Nat Rev Cancer. 2015; 15:701–11. [PubMed: 26563462]
30. Bolla M, Verry C, Long J-A. High-risk prostate cancer: combination of high-dose, high-precision radiotherapy and androgen deprivation therapy. Curr Opin Urol. 2013; 23:349–54. [PubMed: 23673512]
31. Van Poppel H, Klotz L. Gonadotropin-releasing hormone: an update review of the antagonists versus agonists. Int J Urol. 2012; 19:594–601. [PubMed: 22416801]
32. Hopmans SN, Duivenvoorden WCM, Werstuck GH, Klotz L, Pinthus JH. GnRH antagonist associates with less adiposity and reduced characteristics of metabolic syndrome and atherosclerosis compared with orchiectomy and GnRH agonist in a preclinical mouse model. Urol Oncol. 2014; 32:1126–34. [PubMed: 25242517]
33. Redding TW, Schally AV, Radulovic S, Milovanovic S, Szepeshazi K, Isaacs JT. Sustained release formulations of luteinizing hormone-releasing hormone antagonist SB-75 inhibit proliferation and enhance apoptotic cell death of human prostate carcinoma (PC-82) in male nude mice. Cancer Res. 1992; 52:2538–44. [PubMed: 1568223]
34. Mabjeesh NJ, Willard MT, Frederickson CE, Zhong H, Simons JW. Androgens stimulate hypoxia-inducible factor 1 activation via autocrine loop of tyrosine kinase receptor/phosphatidylinositol 3'-kinase/protein kinase B in prostate cancer cells. Clin Cancer Res. 2003; 9:2416–25. [PubMed: 12855613]
35. Joseph IB, Nelson JB, Denmeade SR, Isaacs JT. Androgens regulate vascular endothelial growth factor content in normal and malignant prostatic tissue. Clin Cancer Res. 1997; 3:2507–11. [PubMed: 9815654]
36. Park S-Y, Kim Y-J, Gao AC, Mohler JL, Onate SA, Hidalgo AA, et al. Hypoxia increases androgen receptor activity in prostate cancer cells. Cancer Res. 2006; 66:5121–9. [PubMed: 16707435]

37. Mitani T, Harada N, Nakano Y, Inui H, Yamaji R. Coordinated action of hypoxia-inducible factor-1α and β-catenin in androgen receptor signaling. J Biol Chem. 2012; 287:33594–606. [PubMed: 22865883]

38. Milosevic M, Chung P, Parker C, Bristow R, Toi A, Panzarella T, et al. Androgen withdrawal in patients reduces prostate cancer hypoxia: implications for disease progression and radiation response. Cancer Res. 2007; 67:6022–5. [PubMed: 17616657]

39. Al-Ubaidi FLT, Schultz N, Egevad L, Granfors T, Helleday T. Castration therapy of prostate cancer results in downregulation of HIF-1α levels. Int J Radiat Oncol Biol Phys. 2012; 82:1243–8. [PubMed: 22284032]

40. Joseph IB, Nelson JB, Denmeade SR, Isaacs JT. Androgens regulate vascular endothelial growth factor content in normal and malignant prostatic tissue. Clin Cancer Res. 1997; 3:2507–11. [PubMed: 9815654]

41. Stewart RJ, Panigrahy D, Flynn E, Folkman J. Vascular endothelial growth factor expression and tumor angiogenesis are regulated by androgens in hormone responsive human prostate carcinoma: evidence for androgen dependent destabilization of vascular endothelial growth factor transcripts. J Urol. 2001; 165:688–93. [PubMed: 11176459]

42. Byrne NM, Nesbitt H, Ming L, McKeown SR, Worthington J, McKenna DJ. Androgen deprivation in LNCaP prostate tumour xenografts induces vascular changes and hypoxic stress, resulting in promotion of epithelial-to-mesenchymal transition. Br J Cancer. 2016; 114:659–68. [PubMed: 26954717]

43. Bolla M, Gonzalez D, Warde P, Dubois JB, Mirimanoff RO, Storme G, et al. Improved survival in patients with locally advanced prostate cancer treated with radiotherapy and goserelin. N Engl J Med. 1997; 337:295–300. [PubMed: 9233866]

44. Horwitz EM, Bae K, Hanks GE, Porter A, Grignon DJ, Brereton HD, et al. Ten-year follow-up of radiation therapy oncology group protocol 92-02: a phase III trial of the duration of elective androgen deprivation in locally advanced prostate cancer. J Clin Oncol. 2008; 26:2497–504. [PubMed: 18413638]

Translational Relevance

Targeting of the androgen receptor pathway is a key therapeutic strategy for prostate cancer (PCa). Androgen deprivation therapy (ADT) is the most effective treatment of metastases and is used as adjunctive therapy in combination with radiation for whole gland ablation of intermediate/high risk cancer. A recent multi-center phase III clinical trial in low-risk PCa patients showed tumor ablation, minimal toxicity and decreased localized progression by WST11 vascular targeted photodynamic therapy (VTP) compared to active surveillance. Transcriptome profiling provided herein shows an up-regulated androgen response pathway following VTP. We hypothesized that targeting this pathway with short-course ADT in combination with VTP should significantly delay tumor growth compared to VTP or ADT monotherapies. Furthermore, because ADT and VTP have already been approved for treatment of PCa, the proposed combination might translate rapidly into the clinic and expand the utility of VTP to populations with higher risk, localized PCa.

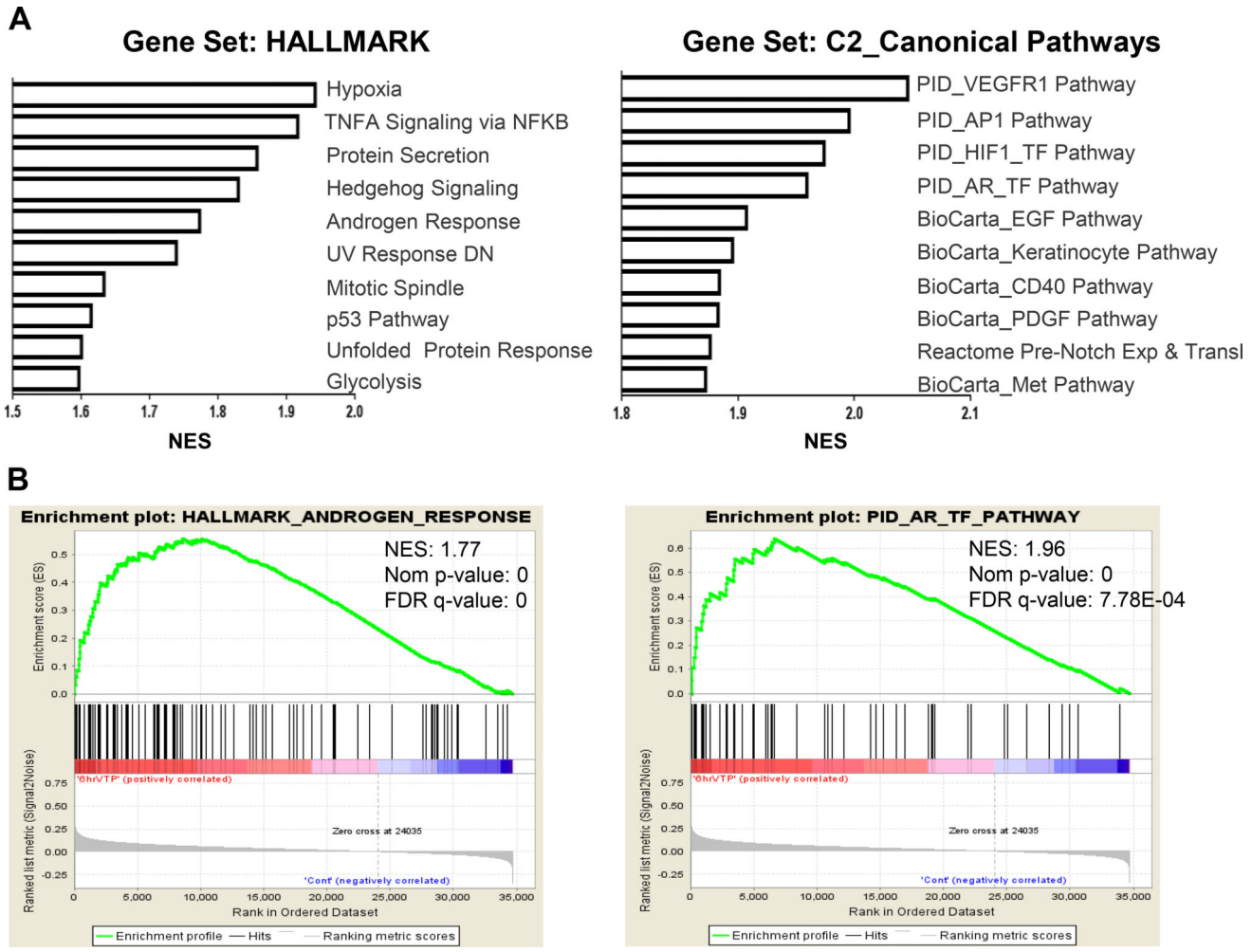

Figure 1. Transcriptome analysis of LNCaP-AR human prostate cancer xenografts post-VTP treatment

(A) Top ranked GSEA pathways among the gene sets HALLMARK and Canonical Pathways (C2). (B) Enrichment plots with normalized enrichment scores (NES) for androgen response pathways within both gene sets at 6 hr post-VTP (n=4) vs. control (n=4).

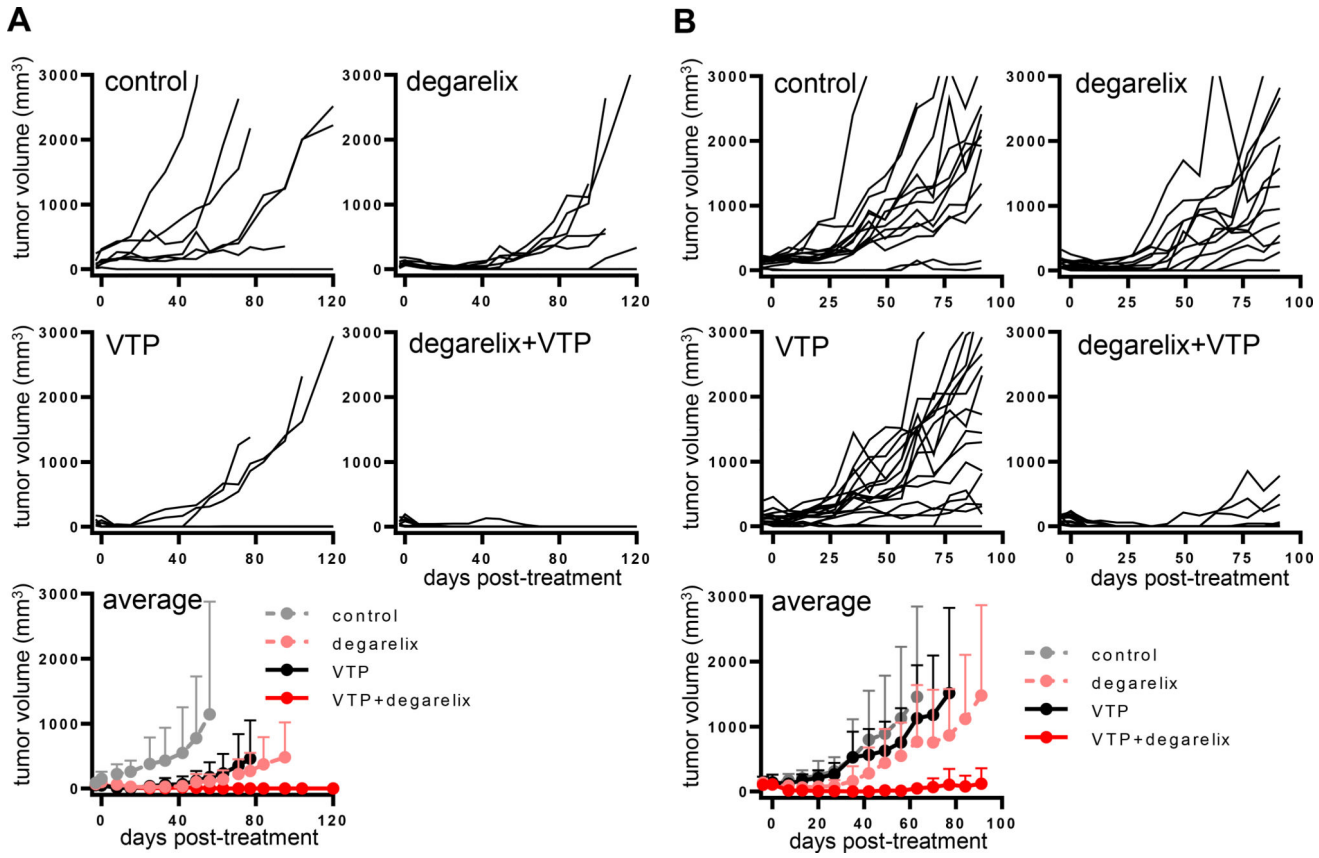

Figure 2. Efficacy of the ADT and VTP combination in the LNCaP-AR human prostate cancer model

(A) Degarelix and VTP combination on tumor growth in athymic nude mice. Mice bearing LNCaP-AR tumors were randomly assigned to 4 cohorts: control (n=7), degarelix (n=9), VTP (n=8), and degarelix + VTP (n=9) and tumor size was measured weekly. The combination treatment suppressed tumor growth more efficiently ($p<0.01$ for combination vs degarelix, $p<0.005$ for combination vs VTP). (B) Combination of degarelix and VTP on tumor growth in SCID mice. Mice bearing LNCaP-AR tumors were randomly assigned to 4 cohorts: control (n=14), degarelix (n=14), VTP (n=17) and degarelix + VTP (n=16) and tumor size was measured weekly ($p<0.0001$, combination vs degarelix or VTP). Results were combined from two separate experiments. One dose of degarelix was given at 3 days prior to VTP.

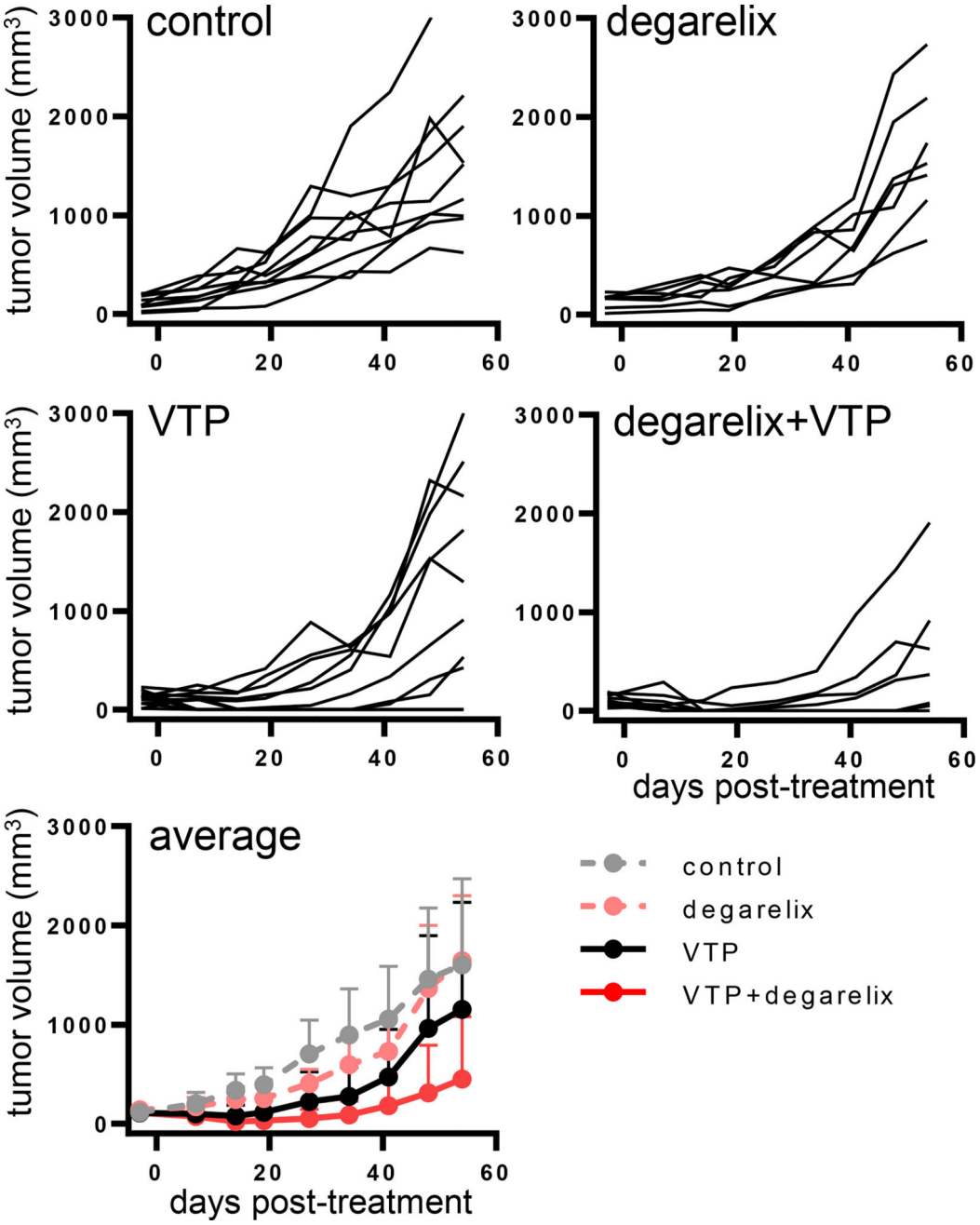

Figure 3. Efficacy of ADT and VTP combination in the VCaP human prostate cancer model

SCID mice bearing VCaP tumors were randomly assigned to 4 cohorts: control (n=7), degarelix (n=9), VTP (n=8), degarelix + VTP (n=9) and tumor size was measured weekly. One dose of degarelix was given 3 days prior to VTP treatment. Combination therapy led to superior local tumor control compared to monotherapy ($p<0.0001$ for degarelix, $p<0.005$ for VTP).

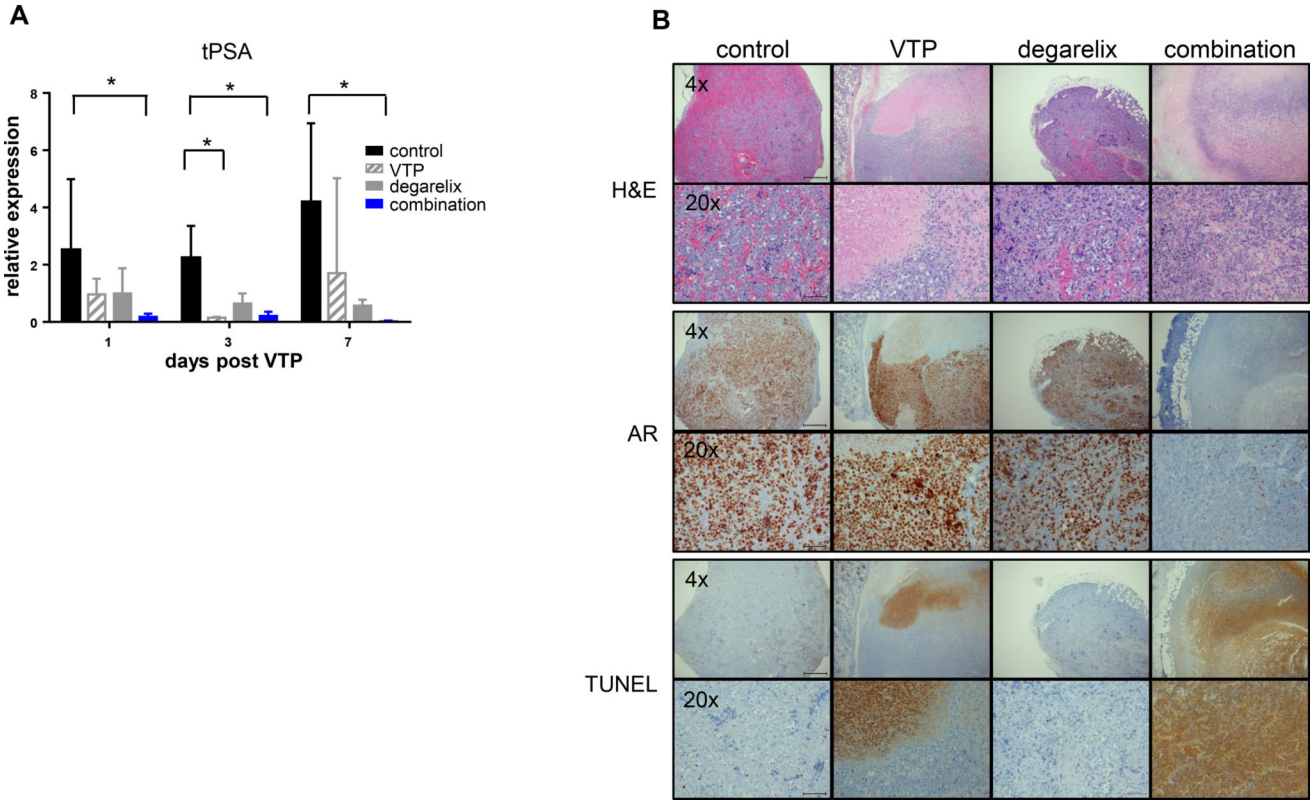

Figure 4. Superior local tumor control by ADT and VTP combination correlated with a decline in serum PSA and intense TUNEL staining

(A) Fold changes of serum tPSA were shown at days 1, 3, and 7 post-VTP. Decrease in PSA level was statistically significant in the mice treated with degarelix/VTP on all three days (* $p<0.05$, ANOVA one way, non-parametric). (B) Histological assessment of degarelix and VTP effects on day 7 post-VTP by H&E, AR and TUNEL. Magnifications of 4x and 20x are shown.

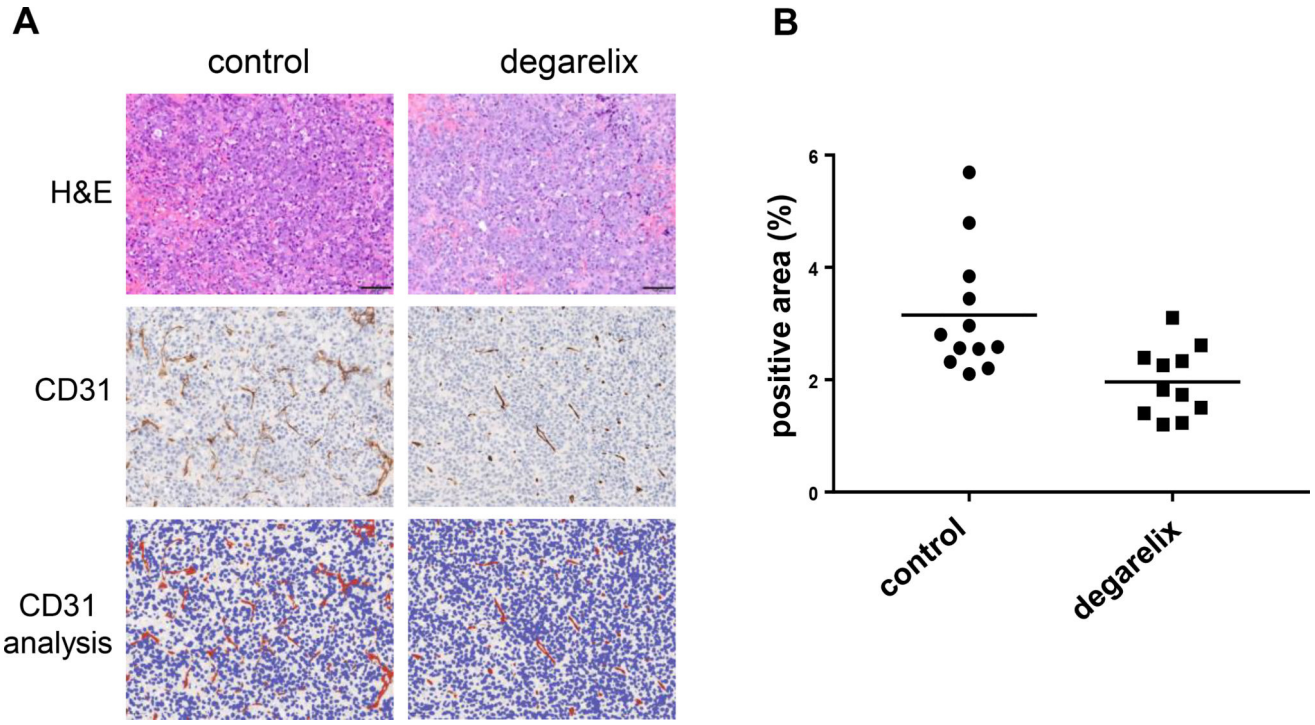

Figure 5. ADT reduces the number of vessels in tumors

(A) A representative H&E and CD31 IHC staining in control and degarelix treated tumors, with image analysis showing positive pixels in red. (B) The quantification of CD31 positive areas in the control group (n= 12) and the degarelix treated group (n=11) are shown. Degarelix resulted in a 38% decrease in CD31staining area compared to controls ($P<0.05$). Image analysis was performed using QuPath software.